NANO LETTERS

2008
Vol. 8, No. 5
1423-1428

Phonon Dispersion and Nanomechanical Properties of Periodic 1D Multilayer Polymer Films

W. Cheng,[†] N. Gomopoulos,[†] G. Fytas,[*,†,‡] T. Gorishnyy,[§] J. Walish,[§] E. L. Thomas,[§] A. Hiltner,[||] and E. Baer[||]

Max Planck Institute for Polymer Research, P.O. Box 3148, 55128 Mainz, Germany, Department of Materials Science & F.O.R.T.H., P.O. Box 1527, 71110 Heraklion, Greece, Department of Materials Science and Engineering, MIT, Cambridge, Massachusetts, 02139, and Department of Macromolecular Science, Case Western Reserve University, Cleveland, Ohio 44106-7202

Received January 31, 2008; Revised Manuscript Received March 4, 2008

ABSTRACT

We report on the first systematic study of phonon propagation in nanostructured composite polymer multilayer films as a function of periodicity and composition using Brillouin light scattering and numerical simulations. The high sensitivity of phonon dispersion to structure and composition allows the probing of the mechanical properties down to the single-layer level. We observe a strikingly different dependence of the longitudinal and shear moduli on confinement effects in the polymer nanolayers. In addition, temperature dependent measurements of sound velocities reveal the presence of distinct glass transition temperatures, indicative of phonon localization in films with large layer thicknesses in agreement with theoretical predictions.

Layer-multiplying coextrusion[1–3] of incompatible polymers can lead to nanostructured multilayer composite films with superior characteristics, such as improved barrier and thermal and mechanical behavior, which are important to many industry applications including coating and packaging. These multilayer films represent a well-defined 1D periodic structure that consists of hundreds to thousands of thin layers of the two component polymers stacked in a strictly alternating fashion. It has also been shown that by properly designing the periodicity and selectively introducing optical anisotropy to these nanolayers, the resulting film can display extraordinary optical effects,[3] e.g., broadband omnidirectional reflection, implying widespread potential applications in optics. The significant practical relevance of such multilayer films demands an advanced control over the film quality, which is however highly influenced by the complex structural relaxation characteristic to polymers. For small layer thickness, in addition to the detailed processing conditions, the chain dynamics is further complicated by other factors including finite-size and interface effects.[4,5] As the mechanical properties of a glassy polymer are susceptible to structural relaxation difference during processing, there is a strong desire to probe the mechanical properties of these multilayer films down to the single-layer level.

The periodic structure of these films deserves special attention as studies on photonic[6] and phononic crystals[7] have revealed the potential of periodically structured composite materials in manipulating classical waves. One of the pivotal concerns for the current system is the phonon dispersion behavior. As phonons in dielectric materials play a decisive role for heat transport, a good knowledge of phonon propagation in such structured materials is the precondition to finally realize heat management by structure engineering.[8] The multilayered structure with periodicity commensurate to the wavelength of the visible light may allow the occurrence of confinement-induced enhancement of photon−phonon interactions,[9,10] an effect sensitive to phonon dispersion as well. Moreover, phonon dispersion behavior is essentially determined by the elastic parameters and the structure of the system. Therefore, it provides valuable details on the structure modulation of phonons and the mechanical properties of the individual layers. The latter suggests that the desired quality control of the multilayer films can be achieved by monitoring the phonon propagation in the film. Knowledge on phonon attenuation could further provide information such as structural relaxation and material defects.[11] In spite of the great importance of phonon dispersion

* Corresponding author. E-mail: fytas@mpip-mainz.mpg.de.
[†] Max Planck Institute for Polymer Research.
[‡] Department of Materials Science & F.O.R.T.H.
[§] Department of Materials Science and Engineering, MIT.
[||] Department of Macromolecular Science, Case Western Reserve University.

10.1021/nl080310w CCC: $40.75
Published on Web 03/26/2008

in such polymeric nanostructured films with 1D periodicity, the only experimental study so far was performed recently on a film composed of alternating poly(methylmethacrylate) (PMMA) and poly(ethylene terephthalate) (PET) nanolayers using Brillouin light scattering (BLS),[12] which probes phonon dispersion via inelastic scattering of light by phonons. Although this preliminary attempt clearly revealed the layer confinement of phonon propagation as well as the impressive mechanical anisotropy, the single film used with strong optical anisotropy excluded a deep insight into such a system.

In this work, by applying BLS to a series of layer-multiplying coextruded free-standing films composed of alternating poly(carbonate) (PC) and poly(methylmethacrylate) (PMMA) nanolayers, we report on the first systematic experimental investigation of the evolution of the phonon dispersion relation with composition and periodicity in such polymeric 1D periodic structures. We observed a drastic increase in complexity of the dispersion relation as the lattice constant d becomes comparable to the phonon wavelength and found a good general match with simulation by finite element analysis (FEA) using no fitting parameters. As opposed to delocalized phonons in films with small layer thickness h, spontaneous existence of both layer-confined and delocalized phonons was observed for films with large h. Taking advantage of the good optical isotropy of the film and the different glass-transition temperature (T_g) of PC and PMMA, we successfully identified the distinct nature of many propagation phonons by monitoring the polarization of the scattered light and the temperature dependence of phonon-phase velocities. Further, by varying the periodicity d while keeping the composition constant, the observed sharp contrast between the d-insensitive and -sensitive phonons, with longitudinal and transverse polarization, respectively, clearly reveals the different impact of confinement effects on longitudinal and shear moduli of the film. While the former remains constant, the latter shows an apparent increase with decreasing h. These findings are not limited to 1D systems but rather illustrate qualitatively general features of wave propagation and mechanical behavior in polymeric periodic nanostructures.

The PC/PMMA multilayer films of total thickness about 50 μm with different periodicity and composition were fabricated by varying the layer-multiplying number and the volume fractions ϕ of the pure components.[1,2] BLS was employed for the direct measurement of the phonon dispersion relations. This technique records the spectrum $I(\mathbf{q}, \omega)$ of light scattered inelastically by thermal phonons propagating in the sample. Here, $\mathbf{q}$ is the scattering wave vector defined by the wave vectors of the incoming and scattered photons as $\mathbf{q} = \mathbf{k}_i - \mathbf{k}_s$, and ω is the frequency shift of the scattered light. For homogeneous media, the momentum conservation requires that $\mathbf{q} = \mathbf{k}$, where $\mathbf{k}$ is the wave vector of the acoustic phonon involved in the scattering process. The frequency shift is given by $\omega = \pm ck$ as a result of energy conservation, where c is the phase velocity of the phonon with longitudinal or transverse or mixed polarizations. A high-resolution six-pass tandem Fabry–Perot interferometer and a light scattering setup[12] allowing both $\mathbf{q}$ and temperature

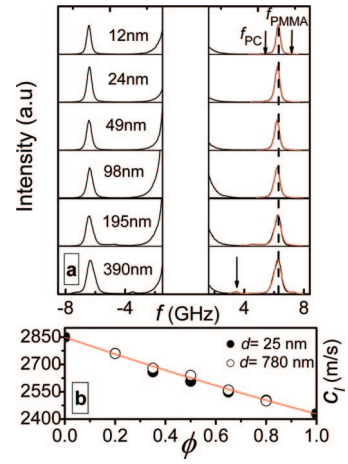

Figure 1. (a) Isotropic (VV) BLS spectra at $q_{||} = 0.0152$ nm^{-1} and 20 °C for six periodic PC/PMMA multilayer films with symmetric composition but different layer thickness as stated in the plot. The two arrows on the top of the figure denote the frequency of the longitudinal phonon at 0.0152 nm^{-1} in the pure PC (f_{PC}) and PMMA (f_{PMMA}) multilayer films. The arrow indicates the presence of additional spectral component in the film with $h = 390$ nm. (b) Longitudinal sound velocity c_l is plotted as a function of PC composition in the PC/PMMA multilayer films with bilayer spacing $d = 25$ nm (solid symbols) and $d = 780$ nm (open symbols). The solid line denotes the representation by Wood's relation.[14]

variations were employed to record the spontaneous Brillouin spectrum at hypersonic (1–50 GHz) frequencies. Choosing the polarization of the incident laser beam perpendicular (V) to the scattering plane (sagittal plane) and selecting the polarization of the scattered light either vertical (V) or parallel to the scattering plane, both polarized (VV) and depolarized (VH) spectra can in principle be recorded. Temperature-dependent measurements were done by placing the sample into a heating chamber, and the sample was heated up from room temperature to 140 °C by multiple steps. At every given temperature, the sample was stabilized for about 15 min before the beginning of the measurements. Then BLS data were acquired for about 30 min for each scan. In the present study, BLS was used in the transmission scattering geometry[12,13] such that the scattering angle is twice the reflection angle α (see Supporting Information Figure S1a). In this case, the scattering wave vector $\mathbf{q}$ is parallel to the layers with magnitude $q_{||} = (4\pi/\lambda) \sin \alpha$ independent of the refractive indices of the layers, where $\lambda = 532$ nm. Figure 1a shows polarized (VV) Brillouin spectra at $q_{||} = 0.0152$ nm^{-1} and ambient conditions for six PC/PMMA films with symmetric composition ($\phi = 0.5$) but different layer thickness between 12 and 390 nm. For a better visualization, the central elastic line due to the reference laser beam (used to stabilize the tandem Fabry–Perot interferometer) was omitted over the frequency range ±1.3 GHz around $f = 0$ GHz.

All spectra show a prominent Brillouin doublet surprisingly at the same frequency in the BLS spectra of Figure 1a. The peak frequency $f = 6.35$ GHz at $q_{||} = 0.0152$ nm^{-1} leads to the phase velocity ($c_l = 2\pi f/q_{||}$) 2625 ± 30 m/s for the phonon with longitudinal polarization. This value falls between the longitudinal sound velocities of the two materials ($c_{lPMMA} = 2850 \pm 40$ m/s and $c_{lPC} = 2430 \pm 30$ m/s)

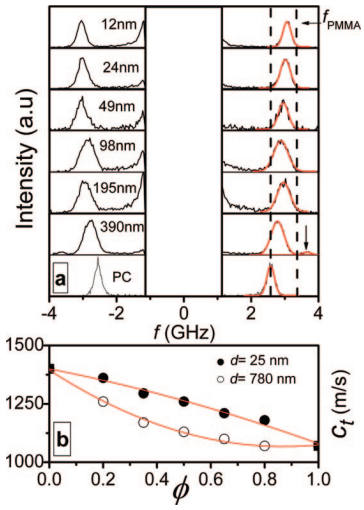

Figure 2. (a) Anisotropic (VH) BLS spectra at $q_{||} = 0.0152$ nm^{-1} and 20 °C for pure PC film and six periodic PC/PMMA multilayer films with symmetric composition but different layer thickness as stated in the plot. The two vertical lines denote the frequency of the shear phonon at 0.0152 nm^{-1} in the pure PC (dashed) and PMMA (f_{PMMA}) multilayer films. The arrow indicates the presence of additional spectral component in the film with $h = 390$ nm. (b) Shear sound velocity is plotted as a function of PC composition in the PC/PMMA multilayer films with bilayer spacing $d = 25$ nm (solid symbols) and $d = 780$ nm (open symbols).

measured in pure PMMA and PC films coextruded under the same condition. Assuming a homogeneous ($hq_{||} < 1$) two-component medium, application of Wood's law[14] to estimate the sound velocity in a PC/PMMA composite with PC volume fraction $\phi = 0.5$ yields $c_{eff} = 2615$ m/s, in excellent agreement with the experimental value of c_l. The appearance of this distinct longitudinal phonon propagating with the same velocity in all six films indicates an effective-medium behavior for all these films, which is rather unexpected for the three films with large layer thickness and hence $hq_{||} > 1$. For the latter, a closer inspection of the spectra in Figure 1a indeed reveals additional spectral features, e.g., a broader line shape of the main peak and a second spectral line indicated by the arrow (see Figure 3 below). A homogeneous-medium-like behavior is also observed for the PC/PMMA multilayer films at constant periodicity d but different compositions. Figure 1b displays the effective-medium longitudinal phonon velocity for five different PC volume fraction ϕ with two extreme periodicities, $d = 25$ nm and $d = 780$ nm. The solid line is the prediction of the Wood's law[14] with no adjustable parameters. The data suggest that the confinement of PC and PMMA layers at nanoscale does not affect the longitudinal modulus, $M = \rho c_l^2$, of the multilayer films assuming a constant density ρ.

Figure 2a displays the depolarized (VH) spectra at $q_{||} = 0.0152$ nm^{-1} for the same six films of Figure 1 including the coextruded pure PC "multilayer". Because the intensity of the VH spectrum is proportional to the segmental optical polarizability anisotropy,[15] the VH spectrum of the pure PMMA "multilayer" film is hardly measurable. The glassy films support shear, and hence the single Brillouin doublet in the VH spectrum is assigned to the phonon with transverse polarization. For the pure PC glassy film, the transverse

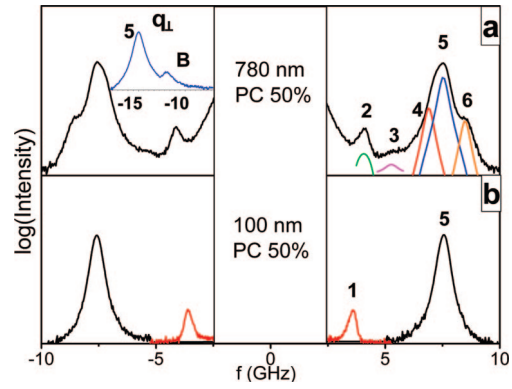

Figure 3. BLS spectra at $q_{||} = 0.0181$ nm^{-1} and 20 °C for two periodic symmetric multilayer films with bilayer thickness $d = 780$ nm (a) and 100 nm (b). The numbers indicate modes with increasing frequency. Modes (**1**) and (**5**) are the transverse and longitudinal phonons in the VH (in b) and in Figure 2) and VV (Figure 1) spectra. The inset in (a) shows the isotropic spectrum of this film at $q_\perp = 0.035$ nm^{-1} perpendicular to the layers where (**B**) is the "Bragg" phonon. The spectra are well represented by a sum of up to five Lorentzian lineshapes as shown by the solid lines in (a).

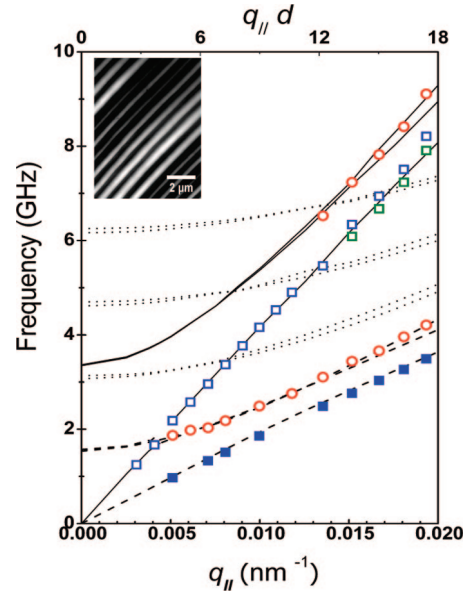

Figure 4. The dispersion relations for a symmetric film having a bilayer thickness $d = 780$ nm. The lines indicate the theoretical dispersions for the modes with quasilongitudinal (QL) (solid) quasitransverse (QT) (dashed) and mixed (dotted) polarizations. Open and solid symbols refer to the isotropic (VV) and anisotropic (VH) BLS respectively. Cross sectioned TEM image of this multilayer film is shown in the inset.

sound velocity c_{tPC} amounts to 1070 m/s, whereas for PMMA, the value of $c_{tPMMA} = 1400$ m/s was obtained from the VH spectrum of a bulk PMMA sample. In clear contrast to the VV spectra of Figure 1a, the peak position for the symmetric PC/PMMA multilayers is no longer constant but shifts to higher frequencies with decreasing layer thickness. By monitoring the q-dependence of the spectrum, this transverse phonon is found to show a linear dispersion (see Figure 4 below) for all six films like the longitudinal phonon in Figure 1. Therefore all films exhibit effective-medium behavior for the transverse phonon propagation. However, the transverse sound velocity shows a monotonic increase

from 1130 m/s for the largest layer thickness ($h = 390$ nm) to 1270 m/s for the thinnest layer ($h = 12$ nm).

To further verify this finding, we also measured the VH spectra for the films with two extreme periodicities and five different compositions. The same effective-medium and linearly dispersed transverse phonons are found in all the films, and the increased shear modulus with decreasing layer thickness is confirmed as well for asymmetric compositions, as shown in Figure 2b. Thus it is clearly revealed that the confinement effect has an evident impact on the shear modulus of these films despite its negligible influence on the longitudinal modulus, possibly due to the confinement-induced stronger shearing force on polymer chains during processing. This impacts the chain conformation more than the packing density. An analog to the Wood's relation is, however, not known for shear modulus, and the lines in Figure 2b represent a polynomial least-squares fit to the experimental c_t data varying between c_{tPMMA} and c_{tPC} of the pure PMMA and PC, as expected for an effective-medium behavior. The shear modulus, $G = \rho c_t^2$, increases by about 60% in the bilayers with $h_{PC} = 5$ nm compared to the bilayers with $h_{PC} = 624$ nm film ($G = 1.5$ GPa and $\rho = 1.2$ g/cm^3).

In addition to the impressive effective-medium behavior, the recorded BLS spectra also carry important information on the structure influence of the structure on the phonon propagation. For example, by comparing the spectra in Figures 1a and 2a of the films with the largest ($d = 780$ nm) and smallest ($d = 25$ nm) periodicity, one can discern an obviously broadened main peak including the additional spectral lines. For a better visualization of the spectral features, we plotted the VV spectra in logarithmic intensity scale as shown in Figure 3a,b for the two symmetric-composition films with periodicity $d = 780$ nm and $d = 100$ nm, respectively. For the former with larger layer thickness ($h = 390$ nm), the rich features are clearly visualized, and up to five modes (**2**–**6**) are clearly resolved. For the second film with $d = 100$ nm ($h = 50$ nm), the single longitudinal (**5**) and transverse (**1**) modes of Figure 3 display a complete homogeneous-medium behavior. The barely distinguishable VV spectra for films with low $h(hq_{||} < 1)$ and their rich features at high $h(hq_{||} > 1)$ are in agreement with the anticipated interaction between wave and structure.

As a brief digression of the in-plane phonon propagation under discussion, the inset to Figure 3a shows a VV BLS spectrum for phonon propagation normal to the layers recorded at $q_\perp = 0.035$ nm^{-1}. There are two peaks present: peak (**5**) at roughly 15 GHz corresponding to the effective-medium longitudinal phonon and a "Bragg" peak[16] (**B**) at roughly 12 GHz due to the periodicity modified momentum conservation condition in the scattering process (see Supporting Information Figure S1b). The phase velocity of the effective-medium phonon is found to be the same as that for in-plane propagation, indicating the mechanical isotropy of the present system at the long wavelength limit, in contrast to the previously probed PMMA/PET film.[12] The frequency of (**B**) is related to the lattice constant and therefore can be used to estimate d and to also check the possible variation of the layer periodicity over the sample within different probed volumes. We found that d fluctuates about 20% around the nominal 780 nm thickness[1,2] at various film spots (beam diameter $\sim$100 μm), which is consistent with the thickness variations observed with TEM (inset in Figure 4).

The detailed knowledge of the in-plane phonon propagation including the identification of the spectral features in Figure 3 needs the phonon dispersion relation, which is a plot of the BLS peak frequencies versus $q_{||}$, as shown in Figure 4 for the symmetric-composition film with layer thickness 390 nm. The previously encountered effective-medium longitudinal (**5**) and transverse (**1**) phonons are readily identified by their linear dispersion that yields the longitudinal and transverse phase velocities c_l and c_t, respectively. The origin of modes (**2**–**4**) and (**6**) cannot be identified without computation of the theoretical dispersion relations. However, the experimental dispersion of these modes in Figure 4 bears resemblance to layer guided modes,[16,17] suggesting a relation to the multilayer structure. The apparent phase velocities $v(q_{||}) = 2\pi f/q_{||}$ of these "structural" modes fall close to c_t for (**2**, **3**) and to c_l for (**6**).

Finite element analysis (FEA) was used to compute phononic dispersion relations and provide interpretation of the observed propagation modes.[18,19] This model assumes perfectly bonded, ideally flat layers with uniform thickness, no roughness and defects, no spatial variations in elastic properties within a given layer, and zero interface thickness. The following densities and elastic constants were used in the model: $\rho_{PMMA} = 1190$ kg/m^3, $E_{PMMA} = 6.26$ GPa, $\sigma_{PMMA} = 0.341$; $\rho_{PC} = 1300$ kg/m^3, $E_{PC} = 4.11$ GPa, $\sigma_{PC} = 0.38$. These values of elastic constants are based on independent measurements of c_l and c_t in homogeneous PMMA and PC films. Figure 4 shows the comparison of the theoretical dispersion relation and the experimental results for the symmetric-composition film with periodicity $d = 780$ nm, and a good agreement between theory and experiment is found. The predicted quasilongitudinal (QL), quasitransverse (QT), and mixed modes (modes with displacements fields primarily parallel, perpendicular, or without preferential orientation to the wave vector, respectively) are shown as solid, dashed, and dotted lines, respectfully. Note that scattering from mixed modes is generally very weak and difficult to detect experimentally.[18] In fact, there is an overall good agreement between the experimental and modeling results for all the film compositions and periodicities with no adjustable parameters. The appearance of additional modes (**2**–**4**) and (**6**) is predicted by theory. Importantly, FEA allows computing the details of the displacement fields, thereby allowing deeper insight into the nature of these modes.

For small layer thickness ($hq_{||} < 1$), FEA predicts an effective medium behavior for both longitudinal and transverse phonon propagation and the corresponding displacement fields do not show preferred localization in any layer. This is a situation deserving no particular concern, and we are interested in structure induced mode localization. Displacement fields corresponding to QT and QL modes for $q_{||} = 0.025$ nm^{-1} in the symmetric film with $d = 780$ nm are shown in Figure 5, ordered from low to high frequency.

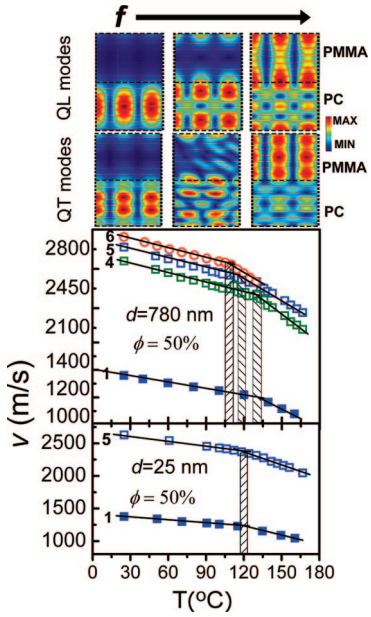

Figure 5. Details of the displacement fields for the quasitransverse and quasilongitudinal modes (in increasing frequency) computed for the symmetric 780 nm bilayer film at $q_{||} = 0.025$ nm^{-1}. The vertical shaded regions indicate the softening transition temperatures for the modes (**1**, **4**–**6**) of the experimental BLS spectrum of Figure 3a. Solid lines represent linear fits of the experimental velocities before and after the transition.

There are three distinct QT (**1**–**3**) and three QL (**4**–**6**) modes predicted for this sample, although only two QT modes are resolved experimentally, probably due to close proximity of the QT modes and/or structural imperfections of the layers. Note that, while the various QL and QT modes propagate with essentially the same respective phase velocities (Figure 4), the displacements are localized primarily within the individual PC or PMMA layers (Figure 5). When the phonon wave vector $q_{||}$ approaches zero, the modes (**2**, **3**, and **6**) present localized, nonpropagating eigenvibrations of the periodic bilayers with zero group velocities and frequencies given by $f = mc_i/d$ (see Supporting Information Figure S2), where $m = 1, 2, ...$, and c_i is either the longitudinal c_l, for (**6**), or transverse c_t, for (**2**, **3**). For the larger values of $q_{||}$, the displacement fields of these modes evolve into layer guided phonons (Figure 5) propagating with group velocities that approach the phase velocities of the medium, as seen in the dispersion relations in Figure 4. The phase velocity $v(q)$ for the QT (**2**, **3**) and the QL (**6**) layer-guided modes for five films, all with $d = 780$ nm but having different compositions was found to fall onto three branches for all the five films. In fact, due to the relatively low mechanical mismatch of the two layers, all layered guided modes should superimpose in the reduced plot $v(q_{||})/c_t$ vs qL where $L = d$ or $d/2$ for modes (**2**) and (**3**), respectively; this trend is also followed by the QL mode (**6**) with $c' c_l$ (see Supporting Information Figure S2).

The biased spatial distribution of the displacement fields for different modes is manifested in their softening temperatures T_s. The phase velocity $c(T)$ of these modes is anticipated to display the characteristic kink at the temperature that corresponds to the T_s of their propagation medium. Thus, the phase velocity $v(T)$ of various phonon modes can be used in combination with the theoretical modeling to provide interpretation on the nature of the observed propagation modes. Figure 5 shows the $v(T)$ for the symmetric bilayer films with periodicity $d = 780$ nm and $d = 25$ nm. The sample with $d = 25$ nm displays a single T_s of 122 °C, which is intermediate between the T_g of the PMMA (105 °C) and PC (140 °C) layers. Thus, phonons propagating in this film do not resolve the presence of individual layers and display a homogeneous medium-like behavior, further supporting the previous conclusion. In contrast, there are three distinct T_s for phonons propagating in the film with $d = 780$ nm. Modes (**1**) and (**4**) have T_s of ~135 °C, which is similar to T_g of PC; mode (**6**) has T_s of ~105 °C, which is essentially the T_g of PMMA, while T_s of mode (**5**) is ~122 °C. Therefore, modes (**1**) and (**4**) must propagate primarily in the PC layers: mode (**6**), primarily in the PMMA layers, and mode (**5**), in both PC and PMMA layers. This conclusion agrees reasonably well with the theoretical displacement fields shown in Figure 5, which suggest that the lowest frequency QT and QL modes (**1**, **4**) should propagate in the PC layers, the higher frequency QL mode (**6**) in the PMMA layers, while the mid-frequency longitudinal mode (**5**) is not strongly localized.

In summary, we report the first systematic study of in-plane phonon propagation in PC/PMMA multilayer films. BLS measurements reveal complex dispersion relations with two or more structure related modes. For periodicities much less than the phonon wavelength, the dispersion relation displays an effective homogeneous medium behavior with the propagation of two phonons with longitudinal and transverse polarization. The confinement in the layered structure impacts only the shear modulus, which was found to increase with decreasing layer thickness. FEA is employed to compute the theoretical dispersion relation and provides a good general agreement with experiment using no fitting parameters. The temperature dependence of the phonon phase velocities is used to identify the nature of the observed propagation modes and provides a measurement of the T_g of the individual polymer nanolayers. The findings in this study will contribute to employing nanostructured materials to manipulate the propagation of elastic waves, which presents a rich area for further research.

Acknowledgment. This material is supported in part by the National Science Foundation under Grant No. DMR 0423914.

Supporting Information Available: Optical path of the incident laser and the scattered light in a two-layer film with refractive indices n_1 and n_2 for a scattering $\theta = 2\alpha$ where α is the angle of incidence ($q_1 = q_2$) . Phase velocity v for the layer guided modes (**2**) and (**3**) vs q for five PC/PMMA bilayer films with $d = 780$ nm and five different (PC) compositions. This material is available free of charge via the Internet at http://pubs.acs.org.

References

(1) Baer, E.; Hiltner, A.; Keith, H. D. *Science* **1987**, *235* (4792), 1015–1022.

(2) Liu, R. Y. F.; Jin, Y.; Hiltner, A.; Baer, E. *Macromol. Rapid Commun.* **2003**, *24* (16), 943–948.
(3) Weber, M. F.; Stover, C. A.; Gilbert, L. R.; Nevitt, T. J.; Ouderkirk, A. J. *Science* **2000**, *287* (5462), 2451–2456.
(4) Bansal, A.; Yang, H. C.; Li, C. Z.; Cho, K. W.; Benicewicz, B. C.; Kumar, S. K.; Schadler, L. S *Nat. Mater.* **2005**, *4* (9), 693–698.
(5) Lee, J. Y.; Su, K. E.; Chan, E. P.; Zhang, Q. L.; Ernrick, T.; Crosby, A. J. *Macromolecules* **2007**, *40* (22), 7755–7757.
(6) Joannopoulos, J. D.; Villeneuve, P. R.; Fan, S. H. *Nature* **1997**, *386* (6621), 143–149.
(7) Sigalas, M.; Kushwaha, M. S.; Economou, E. N.; Kafesaki, M.; Psarobas, I. E.; Steurer, W. *Z. Kristallogr.* **2005**, *220* (9–10), 765–809.
(8) Gorishnyy, T.; Maldovan, M.; Ullal, C.; Thomas, E. *Phys. World* **2005**, *18* (12), 24–29.
(9) Dainese, P.; Russell, P. S. J.; Joly, N.; Knight, J. C.; Wiederhecker, G. S.; Fragnito, H. L.; Laude, V.; Khelif, A. *Nat. Phys.* **2006**, *2* (6), 388–392.
(10) Trigo, M.; Bruchhausen, A.; Fainstein, A.; Jusserand, B.; Thierry-Mieg, V *Phys. Rev. Lett.* **2002**, *89*, 227402.
(11) Priadilova, O.; Cheng, W.; Tommaseo, G.; Steffen, W.; Gutmann, J. S.; Fytas, G. *Macromolecules* **2005**, *38* (6), 2321–2326.
(12) Cheng, W.; Gorishnyy, T.; Krikorian, V.; Fytas, G.; Thomas, E. L. *Macromolecules* **2006**, *39* (26), 9614–9620.
(13) Cheng, W.; Wang, J. J.; Jonas, U.; Fytas, G.; Stefanou, N. *Nat. Mat.* **2006**, *5* (10), 830–836.
(14) $1/\rho c^2 = \phi/\rho_{PC}c^2_{PC} + (1-\phi)/\rho_{PMMA}c^2_{PMMA}$ with $c_{PC} = (2430 \pm 30)$ *m/s* and $c_{PMMA} = (2850 \pm 40)$ *m/s* assuming the same densities $\rho = \rho_{PC} = \rho_{PMMA}$.
(15) Berne, B.; Pecora, R., *Dynamic Light Scattering with Applications to Chemistry, Biology and Physics*; Dover Publications: New York, 2000.
(16) Urbas, A. M.; Thomas, E. L.; Kriegs, H.; Fytas, G.; Penciu, R. S.; Economou, L. N *Phys. Rev. Lett.* **2003**, *90*, 108302.
(17) Forrest, J. A.; Rowat, A. C.; Dalnoki-Veress, K.; Stevens, J. R.; Dutcher, J. R. *J. Polym. Sci., Part B: Polym. Phys.* **1996**, *34* (17), 3009–3016.
(18) Gorishnyy, T.; Ullal, C. K.; Maldovan, M.; Fytas, G.; Thomas, E. L. *Phys. Rev. Lett.* **2005**, *94* (11), 115501.
(19) Jang, J. H.; Ullal, C. K.; Gorishnyy, T.; Tsukruk, V. V.; Thomas, E. L. *Nano Lett.* **2006**, *6* (4), 740–743.

NL080310W